ISSN: 2664-9640

Modeling and Simulation of Winding Bearingless Brushless DC Motor with 12 Slots / 6 Poles

Panchao Lu *, Wenshao Bu

School of Electrical Engineering, Henan University of Science and Technology, Luoyang 471023, China

Corresponding Author: Panchao Lu

Abstract

In view of the problems in dual-winding bearingless brushless direct current motor (BL-BLDC) such as low power density and the serious electromagnetic coupling caused by the energization between the torque winding of the same tooth and the magnetic suspension winding at the same time, a single winding BL-BLDC with 12 stator slots and 6-pole permanent magnet rotor is studied in this paper. Firstly, the structure of the single winding BL-BLDC is given, and the generation principle of the radial magnetic suspension force and torque is analyzed; secondly, the mathematical model of magnetic suspension force is established by using the equivalent magnetic circuit method, including the controllable radial magnetic suspension force model and the unbalanced unilateral electromagnetic force mathematical model; finally, the magnetic levitation force model of this motor is simulated by ANSYS Maxwell, and the result obtained by finite element simulation is compared with result obtained by mathematical model. The result by simulation shows the validity and correctness of the result by mathematical model for the magnetic levitation force.

Keywords

Bearingless brushless direct current motor; single winding; 12 slots/6 poles; finite element simulation.

1. Introduction

The bearingless motor is a new type of motor that integrates rotary drive and rotor self-suspension functions developed in the past 20 years. It uses the similarity between the magnetic bearing structure and the stator structure of the AC motor to produce magnetic bearings. The winding of the radial force is superimposed on the stator winding of the AC motor, which can simultaneously generate the rotational driving torque of the rotor and the radial magnetic levitation force that controls the suspension of the rotor [3-8]. The bearingless motor not only has all the advantages of the magnetic suspension bearing motor, but also overcomes many of its limitations, so it is more suitable for high-speed rotation driving occasions, such as the high-speed driving of machine tool spindles, the sealed transmission of toxic and hazardous materials in the chemical industry, and the inertia wheel in the aerospace industry. , Artificial heart assist devices in the field of life sciences, turbomolecular pumps in the civil industry, high-speed flywheel energy storage devices, etc. [1, 2, 9-15].

At present, domestic research on BL-BLDC mainly adopts the dual-winding structure, and scholars at home and abroad have also done a lot of research work in this area [1, 2, 9-15]. Literature [15] proposed short-pitch dual windings without calculation based on the finite element method. Analysis results of the torque and suspension force of the bearing motor. Literature [16-18] proposed a 12/6 slot-to-pole ratio single-winding bearingless brushless DC motor and its inverter circuit, and analyzed the principle of the magnetic levitation system,

ISSN: 2664-9640

which can effectively improve the radial magnetic levitation force; The amplitude of the controllable magnetic levitation force in the direction of the vertical coordinate axis is not equal, and in the current torque winding, only some of the coils are active. Compared with the double winding BL-BLDC, the motor power density is increased limited; at the same time, the radial direction is not given. Analytical mathematical model of magnetic levitation force.

Literature [19] proposed a bearingless motor (BELM) radial position control method based on d-q axis current control and integrated winding arrangement. At the same time, in order to simplify the structure of the traditional BELM, it also proposed the integration of two windings. Domestically, for the dual-winding structure BL-BLDC, the literature [1] summarizes the key technologies of bearingless brushless DC motors in detail, and provides a reference for further research on bearingless brushless DC motors. Literature [2] proposed a bearingless brushless DC motor for small water pumps, introduced its structure, the principle of magnetic levitation and the strategy of magnetic levitation control, and carried out the model simulation and magnetic levitation performance of the bearingless brushless DC motor. Test trial. Literature [5] starts from the structure of the bearingless brushless DC motor, elaborates its working principle and establishes an equivalent magnetic circuit; the permanent magnet magnetomotive force is equivalent to the virtual current on the suspension force winding, and the precise diameter is established. The mathematical model of the suspension force is verified by finite element simulation, which provides a theoretical basis for reducing the complexity of the bearingless brushless DC motor system and improving the control accuracy.

The dual-winding BL-BLDC structure has shortcomings. 1) The existence of independent suspension windings reduces the slot ratio of the suspension windings and reduces the power density of the motor; 2) If the torque winding and the suspension winding are energized at the same time, it will cause the torque winding and the magnetic suspension control winding to be energized. Severe electromagnetic coupling between. In view of the shortcomings of dual-winding motors, the use of single-winding BL-BLDC is the inevitable trend of future development.

Aiming at the problems of dual-winding motors, this paper studies the single-winding BL-BLDC structure and the principle of magnetic levitation and torque generation, establishes an accurate mathematical model based on the principle, and conducts finite element simulation; the simulation results verify the correctness of the suspension force model of the structure.

2. Single winding BL-BLDC structure and principle

2.1. Single winding motor structure

Figure 1 is a 12/6 slot pole ratio single winding BL-BLDC structure (winding) distribution structure. This model has 12 stator slots and 6 permanent magnet rotor poles. The motor adopts an inner rotor structure, and 6 permanent magnets are evenly placed on the outer surface of the rotor [9-11].

The N-S pole arrangement is shown in the figure. The stator only winds one type of short-pitch coil, and all the coils are divided into two groups, which are connected in series. One is the U1-V1-W1 coil group, composed of U1+, V1+, W1+, U1-, V1-, W1- coils, and the other is the U2-V2-W2 coil group, including U2+, V2+, W2+, U2-, V2 -, W2-coil. Each coil is independent of each other and is wound on the corresponding stator teeth in turn. According to the change of the rotor angular position, the electromagnetic torque and radial suspension force are alternately generated by changing the current direction of each group of coils.

ISSN: 2664-9640

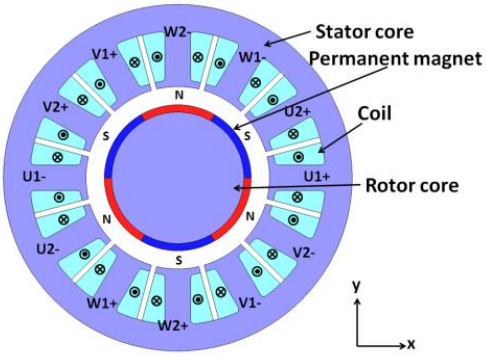

Figure 1: Schematic diagram of 12/6 single winding BL-BLDC model.

2.2. Principle of suspension force generation

Figure 2 is a schematic diagram of the levitation force generation principle of a single winding BL-BLDC with a 12/6 slot pole ratio. When a group of coils is excited, the direction of electromagnetic force generation is the same as the direction of the magnetomotive force of the excited levitation coil, and the net resultant force of the electromagnetic force generated by each phase supports the stable operation of the rotor. Assuming the position of the rotor is shown in Figure 2, Fxu is generated by the excited U1+ and U1- coils, Fxv is generated by the excited V1+ and V1- coils, and Fxw is generated by the excited W1+ and W1- coils. The net levitation force Fx is the vector sum of Fxu, Fxv and Fxw in the x direction; by adjusting the direction and magnitude of the current in the U1-V1-W1 coil group, any levitation force can be generated.

In the same way, the U2-V2-W2 coil group can also generate levitation force. When the N-S boundary of the rotor is located at the edge of the stator teeth, the suspension coil starts to be excited. And while the permanent magnet (PM) facing the stator teeth (with excitation coil) has the same polarity, the suspension coil will continue to be excited. The levitation force can be continuously generated by two coil groups (U1-V1-W1 and U2-V2-W2), which are alternately excited at different rotor angular positions.

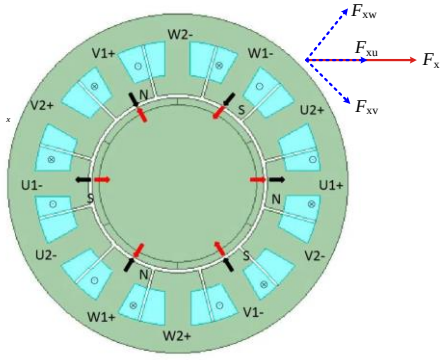

Figure 2: Principle diagram of suspension force generation

2.3. Principle of torque generation

Figure 3 shows the principle of 12-6 single-coil BL-BLDC rotation torque generation. As a specific working condition during the rotation of the motor, it shows the principle of counterclockwise torque generation, which is the same as the traditional motor.

ISSN: 2664-9640

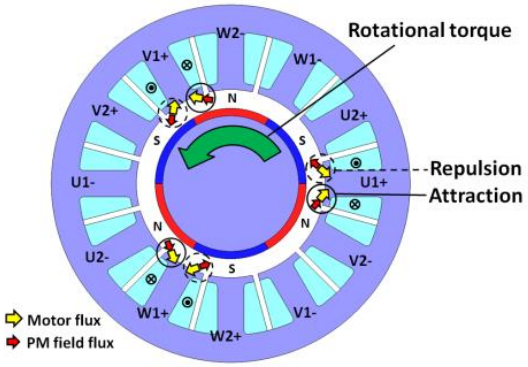

Figure 3: Schematic diagram of torque generation

When the N-pole and S-pole interface overlaps the stator teeth with the excitation coil wound, the N-pole and S-pole and the stator coil generate a pair of attraction and repulsion, respectively, and the combined force of the pair of attraction and repulsion will act on the rotor to produce rotation. Moment. When the U1+, V1+ and W1+ coil groups are excited at the same time, a counterclockwise torque will be generated. When the U1-, V1- and W1- coil groups are excited at the same time, a clockwise torque is generated.

It can be seen that the rotating torque is generated by alternating excitation of the coil groups U1-V1-W1 and U2-V2-W2 at different rotor angular positions, that is, when the torque is generated by the U1-V1-W1 coil group, the levitation force is generated by U2-V2-W2 coil group produces; and when the U2-V2-W2 coil group produces torque, the levitation force is produced by the U1-V1-W1 coil group. Whether the coil group is excited depends on the angular position of the rotor. Therefore, the motor is essentially a time-divided torque and levitation force control motor, in which U1+ and U1-, V1+ and V1-, W1+ and W1- are connected in series respectively, which is the motor's Research on control methods and strategies has brought new directions.

3. Mathematical model and verification of suspension force winding

3.1. Equivalent magnetic circuit method

To analyze the 12-slot 6-pole motor proposed in this paper, firstly, only consider the force of the motor with a single degree of freedom, that is, energize the levitation windings U1+ and U1-, and the motor will generate a levitation force along the axis. Assuming that the thickness of the permanent magnet is, the radius of the inner circle of the stator is, the average air gap length of the motor is, the arc angle of the stator is, the number of turns of the energized winding is N, and the rotor eccentric displacement of the permanent magnet is. In order to facilitate the calculation, in the derivation process Ignoring the core leakage and saturation, neglecting the mutual inductance between the windings, the equivalent magnetic circuit method is used to establish the electromagnetic relationship within the motor. The equivalent magnetic circuit of the U1+ winding is shown in Figure 4.

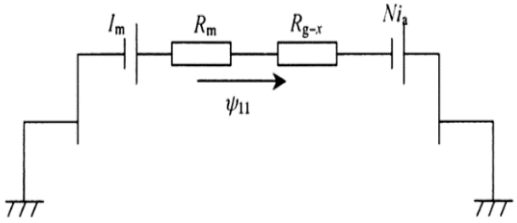

Figure 4: Equivalent magnetic circuit of U1+ winding

ISSN: 2664-9640

The permanent magnet is equivalent to a magnetic flux source, which is the virtual intrinsic magnetomotive force of the permanent magnet, the internal resistance of the permanent magnet, and the total magnetic flux in the equivalent magnetic circuit. According to the Ohm's law of the magnetic circuit, the magnetic flux of the permanent magnet for

$$\phi_{11} = \frac{I_{\mathrm{m}} + Ni_{\mathrm{a}}}{R_{\mathrm{m}} + R_{\mathrm{g\text{-}x}}} = \frac{NI_{\mathrm{eq}}}{R_{\mathrm{eq}}} \tag{1}$$

among them $R_{\mathrm{eq}} = \frac{l_{\mathrm{m}} + g - x}{\mu_0 S}$, $I_{\mathrm{eq}} = \frac{I_{\mathrm{m}}}{N} + i_{\mathrm{a}}$, $R_{\mathrm{m}} = \frac{l_{\mathrm{m}}}{\mu_0 S}$, μ_0 is the vacuum permeability, S is the effective magnetic flux area of the magnetic circuit. The calculation formula is $S = \frac{\theta_1}{360^{\circ}} \times 2\pi rl$, Since the relative permeability of permanent magnets is slightly greater than 1, air gap reluctance $R_{\mathrm{g\text{-}x}} = \frac{\mathrm{g} - x}{\mu_0 S}$, In the calculation, suppose the permanent magnet's recovery permeability is 1, The permanent magnet is equivalent to a constant magnetic flux source [5], can get

$$I_m = H_c l_m = \frac{B_r l_m}{\mu_0} \tag{2}$$

among them H_c is coercivity, B_r is remanence. The expression of flux linkage in the equivalent magnetic circuit of permanent magnet is

$$\lambda = N\phi_{11} = \frac{N^2 \mu_0 S(\frac{I_m}{N} + i_{\mathrm{a}})}{\mathrm{g} - x + l_{\mathrm{m}}} \tag{3}$$

The self-inductance of the winding is

$$L = \frac{\mathrm{d}\lambda}{\mathrm{d}I_{\mathrm{eq}}} = \frac{N^2 \mu_0 S}{\mathrm{g} - x + l_{\mathrm{m}}} \tag{4}$$

Electromagnetic energy in motors

$$W_{\mathrm{m}} = \frac{1}{2} L I_{\mathrm{eq}}^2 = \frac{1}{2} \frac{N^2 \mu_0 S(\frac{I_m}{N} + i_{\mathrm{a}})^2}{\mathrm{g} - x + l_{\mathrm{m}}} \tag{5}$$

Performing Taylor expansion on and ignoring its higher-order terms can get the following formula:

$$W_{\mathrm{m}} = \frac{1}{2} \frac{N^2 \mu_0 S(\frac{I_m}{N} + i_{\mathrm{a}})^2}{(\mathrm{g} + l_{\mathrm{m}})} [1 + \frac{x}{\mathrm{g} + l_{\mathrm{m}}} + (\frac{x}{\mathrm{g} + l_{\mathrm{m}}})^2] \tag{6}$$

The electromagnetic force in the motor can be expressed as

$$F = \frac{\partial W_{\mathrm{m}}}{\partial x} = \frac{1}{2} \frac{N^2 \mu_0 S\left(\frac{I_m}{N} + i_{\mathrm{a}}\right)^2}{(\mathrm{g} + l_{\mathrm{m}})} \left[\frac{1}{\mathrm{g} + l_{\mathrm{m}}} + \frac{2x}{(\mathrm{g} + l_{\mathrm{m}})^2}\right] \tag{7}$$

3.2. Expression of flow electromagnetic force

Since the radial levitation force of the motor is generated by the energization of the levitation force winding, the magnetic pull force generated by the rotor eccentricity can not be considered in the expression of the current through electromagnetic force of the motor, so the current through electromagnetic force F1 on the U1+ winding is expressed by the formula The items in (7) that have nothing to do with x are as follows

ISSN: 2664-9640

$$F_1 == \frac{1}{2}\frac{N^2\mu_0 S\left(\frac{I_m}{N}+i_u\right)^2}{(g+l_m)^2} = \frac{N^2\mu_0 S\left(I_m/N+i_u\right)^2}{2(g+l_m)^2} \tag{8}$$

The levitation force generated by U1-winding energized has the opposite magnetomotive force, and the levitation force generated by it is recorded as, as follows

$$F_2 = -\frac{N^2\mu_0 S\left(I_m/N-i_u\right)^2}{2(g+l_m)^2} \tag{9}$$

Therefore, the resultant force of the suspension force along the X axis is

$$F_{iu} = F_1 - F_2 = \frac{2SB_r l_m N}{(l_m+g)^2} i_u \tag{10}$$

3.3. Expression of eccentric magnetic tension

When the rotor of the motor has an eccentric displacement, an eccentric magnetic pulling force will be generated inside the motor. From the above derivation, it can be seen that the eccentric magnetic pulling force of the motor along the positive axis is expressed as

$$F_{m11} = \frac{N^2\mu_0 S\left(\frac{I_m}{N}\right)^2}{(l_m+g)^3} x = \frac{B_r^2 l_m^2 S}{\mu_0 (l_m+g)^3} x \tag{11}$$

The eccentric magnetic pull along the negative direction of the axis is

$$F_{m12} = -\frac{N^2\mu_0 S\left(\frac{I_m}{N}\right)^2}{(l_m+g)^3} x = -\frac{B_r^2 l_m^2 S}{\mu_0 (l_m+g)^3} x \tag{12}$$

Therefore, the resultant force of the eccentric magnetic pulling force generated by the suspension force windings U1+ and U1- is:

$$F_{m1} = \frac{2N^2\mu_0 S\left(\frac{I_m}{N}\right)^2}{(l_m+g)^3} x = \frac{2B_r^2 l_m^2 S}{\mu_0 (l_m+g)^3} x \tag{13}$$

Considering that when the motor is eccentric, the force of each stator tooth on the rotor is inconsistent, resulting in the stator tooth force received by the rotor is not zero, the total unbalanced force produced is the magnetic pulling force, as follows

$$F_x = \frac{2B_r^2 l_m^2 S}{\mu_0 (l_m+g)^3}(1+2\cos^2 30^\circ + 2\cos^2 60^\circ)x = \frac{6B_r^2 l_m^2 S}{\mu_0 (l_m+g)^3} x \tag{14}$$

It can be obtained from equation (14) that the unbalanced magnetic pulling force produced by the motor has nothing to do with the current, only related to the eccentric position of the motor rotor, and as the eccentric position of the rotor increases, the value of the unbalanced magnetic pulling force will increase accordingly .

3.4. Calculation of single-degree-of-freedom and multi-degree-of-freedom radial suspension force

The radial levitation force of the motor is the resultant force experienced by the motor in the horizontal direction, including the levitation force in the horizontal direction and the unbalanced magnetic pulling force in the horizontal direction, namely

$$F_u = F_{iu} + F_{xu} = \frac{2SB_r l_m N}{(l_m+g)^2} i_u + \frac{6B_r^2 l_m^2 S}{\mu_0 (l_m+g)^3} x_u = k_{iu} i_u + k_{xu} x_u \tag{15}$$

ISSN: 2664-9640

Among them $k_{iu}=\frac{2SB_r l_m N}{(l_m+g)^2}$, $k_{xu}=\frac{6B_r^2 l_m^2 S}{\mu_0(l_m+g)^3}$。Assuming that the geometric parameters of the 6 permanent magnets in this motor model are exactly the same, and other physical parameters are also the same, so for these 6 permanent magnets and is a fixed value.

Considering the multi-degree-of-freedom radial suspension force in the actual model, it can be seen that for V1+, V1- and W1+, W1-, there are also

$$\begin{aligned} F_v &= F_{iv}+F_{xv} \\ &= \frac{2SB_r l_m N}{(l_m+g)^2} i_v + \frac{6B_r^2 l_m^2 S}{\mu_0(l_m+g)^3} x_v \\ &= k_{iv} i_v + k_{xv} x_v \end{aligned} \tag{16}$$

$$\begin{aligned} F_w &= F_{iw}+F_{xw} \\ &= \frac{2SB_r l_m N}{(l_m+g)^2} i_w + \frac{6B_r^2 l_m^2 S}{\mu_0(l_m+g)^3} x_w \\ &= k_{iw} i_w + k_{xw} x_w \end{aligned} \tag{17}$$

In the same way, the above expression can also be obtained by analyzing the suspension force on the Y axis.

3.5. Calculation formula of suspension force at any angle

When the angle of the motor is 0-30°, 60°-90°, 120°-150°, the U1-V1-W1 phase winding of the motor is turned on to generate the levitation force, and the levitation force generated by it is converted to the coordinate system. It can be expressed as:

$$\begin{bmatrix} F_x \\ F_y \end{bmatrix} = \begin{bmatrix} \cos 0° & \cos 120° & \cos 240° \\ \sin 0° & \sin 120° & \sin 240° \end{bmatrix} \begin{bmatrix} F_{U1+U1-} \\ F_{V1+V1-} \\ F_{W1+W1-} \end{bmatrix} \tag{18}$$

The schematic diagram is as follows

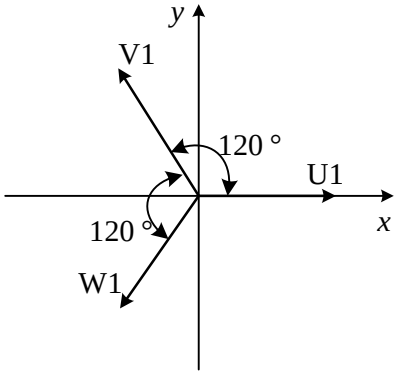

Figure 5: Schematic diagram of U1-V1-W1 coordinates

Substituting into formula (18), we can get

$$\begin{aligned} \begin{bmatrix} F_x \\ F_y \end{bmatrix} &= \begin{bmatrix} \cos 0° & \cos 120° & \cos 240° \\ \sin 0° & \sin 120° & \sin 240° \end{bmatrix} \begin{bmatrix} k_i i_{u1} + k_x u_1 \\ k_i i_{v1} + k_x v_1 \\ k_i i_{w1} + k_x w_1 \end{bmatrix} \\ &= k_i \begin{bmatrix} i_{u1}\cos 0° + i_{v1}\cos 120° + i_{w1}\cos 240° \\ i_{u1}\sin 0° + i_{v1}\sin 120° + i_{w1}\sin 240° \end{bmatrix} + k_x \begin{bmatrix} u_1\cos 0° + v_1\cos 120° + w_1\cos 240° \\ u_1\sin 0° + v_1\sin 120° + w_1\sin 240° \end{bmatrix} \end{aligned} \tag{19}$$

For eccentricity, assume that the eccentricity is $e=\sqrt{x^2+y^2}$,

ISSN: 2664-9640

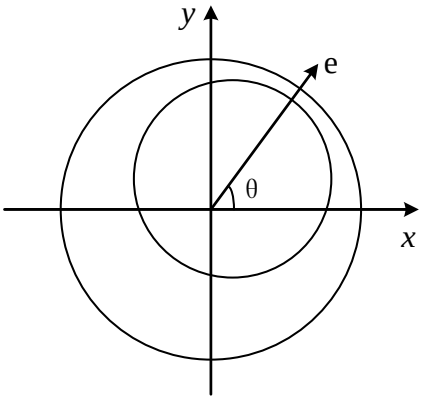

Figure 6: Schematic diagram of rotor eccentricity

At the same time, for any rotor eccentric angle, the eccentricity in the U1-V1-W1 direction and the X-Y coordinate satisfy the following relationship:

$$\begin{aligned} u_1 &= e \cdot \cos\theta \\ v_1 &= e \cdot \cos(120° - \theta) \\ w_1 &= e \cdot \cos(240° - \theta) \end{aligned} \tag{20}$$

(20) Bring in (19) to get

$$\begin{bmatrix} F_x \\ F_y \end{bmatrix} = k_i A_1 + k_x e A_2 \tag{21}$$

Among them

$$A_1 = \begin{bmatrix} i_{u1}\cos 0° + i_{v1}\cos 120° + i_{w1}\cos 240° \\ i_{u1}\sin 0° + i_{v1}\sin 120° + i_{w1}\sin 240° \end{bmatrix},\ A_2 = \begin{bmatrix} \cos 0°\cdot\cos\theta + \cos 120°\cdot\cos(120° - \theta) + \cos 240°\cdot\cos(240° - \theta) \\ \sin 0°\cdot\cos\theta + \sin 120°\cdot\cos(120° - \theta) + \sin 240°\cdot\cos(240° - \theta) \end{bmatrix}$$

A1 and A2 are all intermediate variable matrices.

Similarly, when the angle of the motor is 30°～60°, 90°～120°, 150°～180°, the U2-V2-W2 phase winding of the motor is turned on to generate the levitation force, and the levitation force generated by it is converted The coordinate system can be expressed as:

$$\begin{bmatrix} F_x \\ F_y \end{bmatrix} = \begin{bmatrix} \cos 30° & \cos 150° & \cos 270° \\ \sin 30° & \sin 150° & \sin 270° \end{bmatrix} \begin{bmatrix} F_{U2+U2-} \\ F_{V2+V2-} \\ F_{W2+W2-} \end{bmatrix} \tag{22}$$

The schematic diagram is as follows

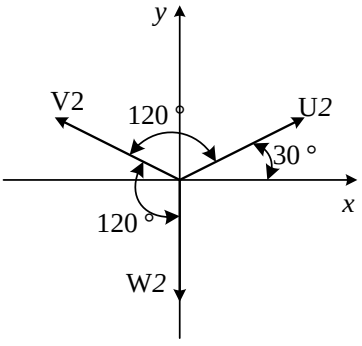

Figure 7: Schematic diagram of U2-V2-W2 coordinates

And have

$$\begin{aligned} u_1 &= e \cdot \cos(30° - \theta) \\ v_1 &= e \cdot \cos(150° - \theta) \\ w_1 &= e \cdot \cos(270° - \theta) \end{aligned}$$

Finally, the expression under this working condition is

ISSN: 2664-9640

$$\begin{bmatrix} F_x \\ F_y \end{bmatrix} = k_i B_1 + k_x e B_2 \tag{23}$$

Among them

$$B_1 = \begin{bmatrix} i_{u2}\cos 30° + i_{v2}\cos 150° + i_{w2}\cos 270° \\ i_{u2}\sin 30° + i_{v2}\sin 150° + i_{w2}\sin 270° \end{bmatrix}$$

$$B_2 = \begin{bmatrix} \cos 30°\cdot\cos(30-\theta) + \cos 150°\cdot\cos(150°-\theta) + \cos 270°\cdot\cos(270°-\theta) \\ \sin 30°\cdot\cos(30-\theta) + \sin 150°\cdot\cos(150°-\theta) + \sin 270°\cdot\cos(270°-\theta) \end{bmatrix}$$

Similar to A1 and A2, B1 and B2 are also intermediate variable matrices.

4. Finite element simulation verification of mathematical model

Aiming at a certain 12-6 single-winding BL-BLDC model, the professional electromagnetic field finite element analysis software Maxwell is used to simulate, and the simulation results are compared with the calculation results of the above mathematical model. In this verification example, the specific prototype related parameters are as follows:

Table 1 Relevant parameters of finite element verification examples

Parameter	Unit	Value
Stator pole arc angle θ	angle	24
Stator inner circle radius r	meter	0.0245
Permanent magnet remanence B_r	Tesla	1.0999
Permanent magnet thickness l_m	meter	0.002
Average air gap length g	meter	0.0005
Number of turns N	---	100

Bring the above parameters into the formula (16) and (17), which can be met by the motor k_i=46.0 N/A, k_x=966.44 N/mm

4.1. Magnetic suspension of magnetic housing in the case of rotor

At this time, when the stator rotation angle θ is satisfied $0 \le \theta < 30$, $60 \le \theta < 90$, $120 \le \theta < 150$

$$\begin{aligned} \begin{bmatrix} F_x \\ F_y \end{bmatrix} &= k_i \begin{bmatrix} i_{u1}\cos 0° + i_{v1}\cos 120° + i_{w1}\cos 240° \\ i_{u1}\sin 0° + i_{v1}\sin 120° + i_{w1}\sin 240° \end{bmatrix} \\ &= k_i \begin{bmatrix} i_{u1} - 0.5 i_{v1} - 0.5 i_{w1} \\ 0.866 i_{v1} - 0.866 i_{w1} \end{bmatrix} \end{aligned} \tag{24}$$

When the indicator rotation angle θ is satisfied $30 \le \theta < 60$, $90 \le \theta < 120$, $150 \le \theta < 180$

$$\begin{aligned} \begin{bmatrix} F_x \\ F_y \end{bmatrix} &= k_i \begin{bmatrix} i_{u2}\cos 30° + i_{v2}\cos 90° + i_{w2}\cos 150° \\ i_{u2}\sin 30° + i_{v2}\sin 90° + i_{w2}\sin 150° \end{bmatrix} \\ &= k_i \begin{bmatrix} 0.866 i_{u2} - 0.866 i_{w2} \\ 0.5 i_{u2} + i_{v2} + 0.5 i_{w2} \end{bmatrix} \end{aligned} \tag{25}$$

In the verification of this example, select the stator rotation angleθ=0°.Set 1A to 10A respectively, with an interval of 1A, iv1= iv1=iw1=0A.

$$\begin{bmatrix} F_x \\ F_y \end{bmatrix} = k_i \begin{bmatrix} i_{u1} \\ 0 \end{bmatrix} \tag{26}$$

Comparing the finite element calculation result with the value derived from the mathematical formula, the value of the X-axis suspension force under different ampere turns is obtained as shown in the figure below:

ISSN: 2664-9640

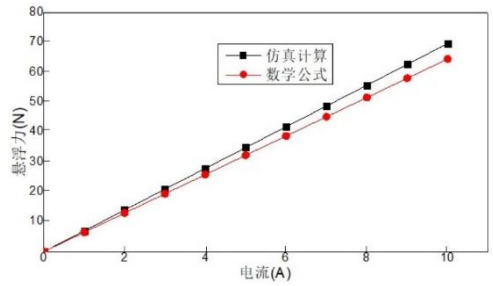

Figure 8: Levitation force vs. current curve

It can be seen from the figure above that the value calculated by the finite element is basically the same as the X-axis suspension force derived from the mathematical formula. As the winding current increases, the X-axis levitation force also increases and becomes a linear relationship, which is consistent with the analysis result of formula (26). At the same time, it can be seen that the error between the Maxwell simulation calculation result and the mathematical formula calculation result is within 5%.

4.2. Analysis of radial magnetic suspension force caused by rotor eccentricity

For the rotation angle condition, formula (23) can be obtained

$$\begin{bmatrix} F_x \\ F_y \end{bmatrix} = k_x eC \tag{27}$$

Among them

$$C = \begin{bmatrix} \cos 0° \cdot \cos 0° + \cos 120° \cdot \cos(120° - 0°) + \cos 240° \cdot \cos(240° - 0°) \\ \sin 0° \cdot \cos 0° + \sin 120° \cdot \cos(120° - 0°) + \sin 240° \cdot \cos(240° - 0°) \end{bmatrix} = \begin{bmatrix} 1.5 \\ 0 \end{bmatrix}$$

C is the intermediate constant matrix, namely

$$\begin{bmatrix} F_x \\ F_y \end{bmatrix} = k_x \mathrm{e} \begin{bmatrix} 1.5 \\ 0 \end{bmatrix} \tag{28}$$

In the verification of this example, given Δx=0.05mm, 0.1mm, 0.15mm, 0.2mm, 0.25mm, 0.3mm; Δy=0mm, compare the results obtained by finite element calculation and mathematical formula calculation, the following can be obtained Picture:

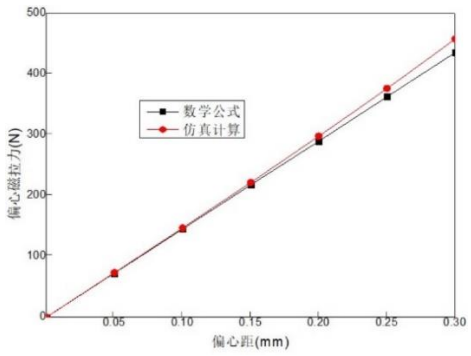

Figure 9: Curve of eccentric magnetic pulling force versus eccentricity

It can be seen from the figure above that the levitation force calculated by the simulation is basically the same as the eccentric magnetic pull force derived from the mathematical formula. With the increase of the eccentricity, the eccentric magnetic force also increases and becomes a linear relationship, which is consistent with the analysis result of formula (28). At the same time, it can be seen that the error between the Maxwell simulation calculation result and the mathematical formula calculation result is within 5%.

ISSN: 2664-9640

5. Conclusion

In view of the low power density of the traditional dual-winding bearingless brushless DC motor (BL-BLDC), if the torque winding and the magnetic levitation winding of the same tooth are energized at the same time, serious electromagnetic coupling and other problems will occur. The single-winding BL-BLDC of a 6-pole permanent magnet rotor has been studied, and the mathematical model of its radial magnetic levitation force has been theoretically deduced. First, through theoretical methods, the principle of generating magnetic levitation force and electromagnetic torque during the operation of a 12/6 slot-to-pole ratio single-winding bearingless brushless DC motor is analyzed; then, the equivalent magnetic circuit method is used to derive The magnetic levitation force analytical mathematical model of the motor of this structure, including the controllable magnetic levitation force model and the unbalanced unilateral electromagnetic tension mathematical model; finally, through the professional electromagnetic field analysis software Ansys Maxwell, the magnetic levitation of the 12/6 slot pole ratio single winding BL-BLDC The force mathematical model was verified and analyzed. The finite element simulation verification results show that the mathematical model of the magnetic levitation force of the single-winding BL-BLDC with 12/6 slot-to-pole ratio proposed in this paper is effective and feasible; it can provide a theoretical basis for the precise control of the structure of the BL-BLDC.

Acknowledgements

This work was supported by Henan Province Science and Technology Research Project (202102210095).

References

[1] Bu W, Huang S, Wan S, et al. General Analytical Models of Inductance Matrices of Four-Pole Bearingless Motors With Two-Pole Controlling Windings[J]. IEEE T MAGN, Vol 14, (2009)No.3

[2] Bu W, Lu P, Lu C, et al. Independent Inverse System Decoupling Control Strategy of Bearingless Induction Motor[J]. Recent Advances in Electrical & Electronic Engineering, Vol 13, (2020)

[3] Bu W, Huang Y, Lu C, et al. Unbalanced displacement LMS extraction algorithm and vibration control of a bearingless induction motor[J]. INT J APPL ELECTROM, Vol l56,(2017) No.1

[4] Bu W, Tu X, Lu C, et al. Adaptive feedforward vibration compensation control strategy of bearingless induction motor[J]. INT J APPL ELECTROM,Vol 63,(2020) No.2

[5] Ooshima M, Miyashita K, Rahman M A. Control circuit topology of a time-divided torque and suspension force control type bearingless motor[C]. *PESGM*, (2012)

[6] Miyashita K, Ooshima M, Uddin M N. Design of a time-divided torque and suspension force control type bearingless motor[C]. *PESGM*, (2011)

[7] Ooshima M, Miyashita K, Nakagawa M. Magnetic levitation tests of a time-divided torque and suspension force control type bearingless motor[C]. *ICEMS*, (2013)

[8] J. Zhu, Z. Q. Deng, X. L. Wang and Q. X. Liao, Principle and Implementation of the Single Winding Bearingless Permanent Magnetic Slice Motor[J], Proceedings of the CSEE, Vol 28, (2008) No.33

[9] L. G. Chen and H. Q. Zhu, An Accurate Mathematical Model of Radial Suspension Force in Bearingless Brushless DC Motors, Proceedings of the CSEE, Vol 32, (2012)

[10] Kobayashi S, Ooshima M, Uddin M N. A Radial Position Control Method of Bearingless Motor Based on d-Q Axis Current Control[J]. IEEE Transactions on Industry Applications, Vol 49 (2013) No.4,P.1827-1835.

ISSN: 2664-9640

[11] Dutta P, Mahato S N. Design of mathematical model and performance analysis of BLBLDC motor[C]. *International Conference on Control. IEEE*, (2014):P.457-461.

[12] Asama J, Mouri A, Oiwa T, et al. Suspension force investigation for consequent-pole and surface-mounted permanent magnet bearingless motors with concentrated winding[C]. *IEEE International Electric Machines & Drives Conference. IEEE*, (February 16, 2016) P.780-785

[13] Zürcher, F, Nussbaumer T, Kolar J W. Motor Torque and Magnetic Levitation Force Generation in Bearingless Brushless Multipole Motors[J]. IEEE/ASME Transactions on Mechatronics,Vol 17 (2012), No.6,P.1088-1097.

[14] Warberger B, Kaelin R, Nussbaumer T, et al. 50-N. m/2500-W Bearingless Motor for High-Purity Pharmaceutical Mixing[J]. IEEE Transactions on Industrial Electronics,Vol 59 (2012), No.5,P.2236-2247.

[15] Reichert T, Nussbaumer T, Kolar J W. Investigation of Exterior Rotor Bearingless Motor Topologies for High-Quality Mixing Applications[J]. IEEE Transactions on Industry Applications, Vol 48 (2013), No.6,P.2206-2216.

[16] Reichert T, Kolar J W, Nussbaumer T. Design study for exterior rotor bearingless permanent magnet machines[C]. *Energy Conversion Congress & Exposition. IEEE*, (2011). P.3377-3382

[17] Reichert, T, Nussbaumer, et al. Bearingless Permanent-Magnet Motor with 4/12 Slot-Pole Ratio for Bioreactor Stirring Applications[J]. Mechatronics, IEEE/ASME Transactions on, (2011).

[18] Sun Y, Yang F, Yuan Y, et al. Out rotor bearingless brushless DC motor for flywheel energy storage[C]. *International Workshop on Complex Systems and Networks (IWCSN)*.(2017).

[19] Reichert, T, Kolar, et al. Stator Tooth Design Study for Bearingless Exterior Rotor PMSM[J]. IEEE Transactions on Industry Applications, Vol 49 (2013),No.4,P.1515-1522.